ELSEVIER

Urologic Oncology: Seminars and Original Investigations 29 (2011) 12–20

UROLOGIC ONCOLOGY

Review article

Modern role of magnetic resonance and spectroscopy in the imaging of prostate cancer

Alessandro Sciarra, M.D.[a,*], Valeria Panebianco, M.D.[b], Stefano Salciccia, M.D.[a], Susanna Cattarino, M.D.[a], Dino Lisi, M.D.[b], Alessandro Gentilucci, M.D.[a], Andrea Alfarone, M.D.[a], Gianna Mariotti, M.D.[a], Roberto Passariello, M.D.[b], Vincenzo Gentile, M.D.[a]

[a] *Department of Urology, University Sapienza, Rome, Italy*
[b] *Department of Radiology, University Sapienza, Rome, Italy*

Received 14 April 2009; received in revised form 2 June 2009; accepted 2 June 2009

Abstract

Recently, a large number of studies have shown that the addition of proton 1H-spectroscopic imaging (1H-MRSI) and dynamic contrast enhanced imaging (DCEMR) to magnetic resonance (MR) could represent a powerful tool for the management of prostate cancer (CaP) in most of its aspects. This combination of MR techniques can substantially sustain the clinical management of patients with CaP at different levels: in particular, (1) in the initial assessment, reducing the need for more extensive biopsies and directing targeted biopsies; (2) in the definition of a biochemical progression after primary therapies, distinguishing between fibrotic reaction and local recurrence from CaP. © 2011 Elsevier Inc. All rights reserved.

Keywords: Prostate neoplasm; Imaging; Magnetic resonance; Spectroscopy

1. Introduction

Prostate cancer (CaP) is one of the most common tumors in the male population. It constitutes about 11% of all male cancers, and it accounts for 9% of all cancer deaths among men [1].

At the moment, the diagnosis of CaP is mainly based on 3 tests: digital rectal examination (DRE), prostate-specific antigen (PSA) value, transrectal ultrasound (TRUS) guided biopsies. The latter is recognized by urologists as the first choice in the diagnosis of prostate pathologies [2]. Although with TRUS the majority of CaP is represented by hypoechoic lesions, only 20% of them are malignant [3]. Moreover, some lesions are isoechoic or appear to have little hypoechogenicity in relation with the surrounding tissue [4]. PSA-value is characterized by low specificity: the Prostate Cancer Prevention Trial stated that no cut-off value distinguishes between CaP and benign disease [5].

All three modern imaging modalities computer tomography, ultrasonography, and magnetic resonance (MR) have been considered to have limitations in the diagnosis of CaP. Recently, many studies [6–9] revealed the high diagnostic accuracy of combined proton 1H-magnetic resonance spectroscopic imaging (1H-MRSI) and dynamic contrast-enhanced imaging MR (DCEMR) in the management of CaP. For a long time, a valid diagnostic imaging procedure has not been available for CaP.

The aim of this article is to review the current role of these new MR-techniques in the early diagnosis, cancer localization, local staging, road map for surgery and radiotherapy, early detection of local recurrence after surgery/radiotherapy, and evaluation of hormonal therapy for CaP.

2. Defining MRSI and DCEMR: Technical aspects

The endorectal MRI is generally performed with a 1.5-T scanner and endorectal coil, filled with 70–90 ml of air on the basis of patient tolerance.

The diagnosis is based on a low signal area within the normal hyperintense peripheral zone on T2-weighted images, or a diffuse unilateral or bilateral hypointensity in the peripheral zone [10].

However, a decreased signal intensity within the high intensity normal peripheral zone can also be attributed to

* Corresponding author. Tel./fax: +39-06-4461959.
E-mail address: a.sciarra@lycos.it (A. Sciarra).

1078-1439/$ – see front matter © 2011 Elsevier Inc. All rights reserved.
doi:10.1016/j.urolonc.2009.06.001

other benign conditions, such as prostatitis, hemorrhage, or hyperplastic nodes [6,11].

The advantage of MRSI is that it suppresses signal contributions from water and fats and provides metabolic informations from substances that are characteristic for the specific tissue [2]. Current sequences examine the prostate in three dimensions with an array of volume elements (voxels) down to 0.25 cm in size [12,13].

In the prostate, the substances analyzed by MRSI are citrate, creatine, and choline. Citrate is produced by healthy prostatic epithelial cells, and it decreases because of energy metabolism in CaP. Creatine is part of the phosphocreatine-creatine system of cellular energy storage. Choline is a cell membrane constituent whose concentrations increase in cases of CaP, as a result of the high turnover. Therefore, citrate levels decrease while creatine and choline levels are increased in CaP [2] (Fig. 1A). For practical purpose, CaP can be distinguished from healthy peripheral zone tissue on the basis of the (Cho + Cr)/Cit ratio [9,11,14]. This ratio includes also polyamines that decrease in CaP. Normal peripheral zone tissue is characterized by voxels with a (Cho + Cr)/Cit ratio < 0.75; cancer is defined as a voxel with (Cho + Cr)/Cit ratio > 0.75 [15]. Unfortunately, some benign conditions, such as prostatitis, postbiopsy hemorrhage, might present an increase of (Cho + Cr)/Cit ratio [16–18]. MRI and MRSI of the prostate can be performed in less than 1 h.

DCEMR can also improve MRI results. It consists in the acquisition of sequential images using T1-weighted sequences during the passage of a contrast agent (gadopentetate dimeglumine) within the prostatic tissue. The technique is based on the assessment of tumor neoangiogenesis, which is an integral feature of tumors. Dynamic imaging parameters are estimated as onset time of signal enhancement, time to peak, peak enhancement, and wash-out [19] (Fig. 1B). The dynamic MR procedure can be performed in 15 min. At this time, in CaP more data in the literature are referred to MRSI than to DCEMRI.

3. CaP detection

3.1. Role of MRSI and DCEMR in the early diagnosis of CaP

Ultrasound-guided biopsy is now the preferred method for histologic diagnosis of CaP. Recent studies have shown a sensitivity, specificity, positive–negative predictive values (PPV and NPV), and diagnostic accuracy of 70%, 89%, 88%, 74%, and 79%, respectively, of combined MRI/MRSI for the diagnosis of CaP in patients with elevated PSA [20]. Bloch et al. [21] investigated 32 patients with a PSA range of 0.99–42.83 ng/ml (mean 3 ng/ml) and a mean age of 65 years, and it referred a diagnostic accuracy of combined MRI/DCEMR of 95%–96% with a sensitivity, specificity, PPV, and NPV of 82%–91%, 95%, 90%–91%, 91%–95%, respectively (Table 1). Several studies analyzed MRSI diagnostic accuracy, comparing it to prostate biopsy. How-

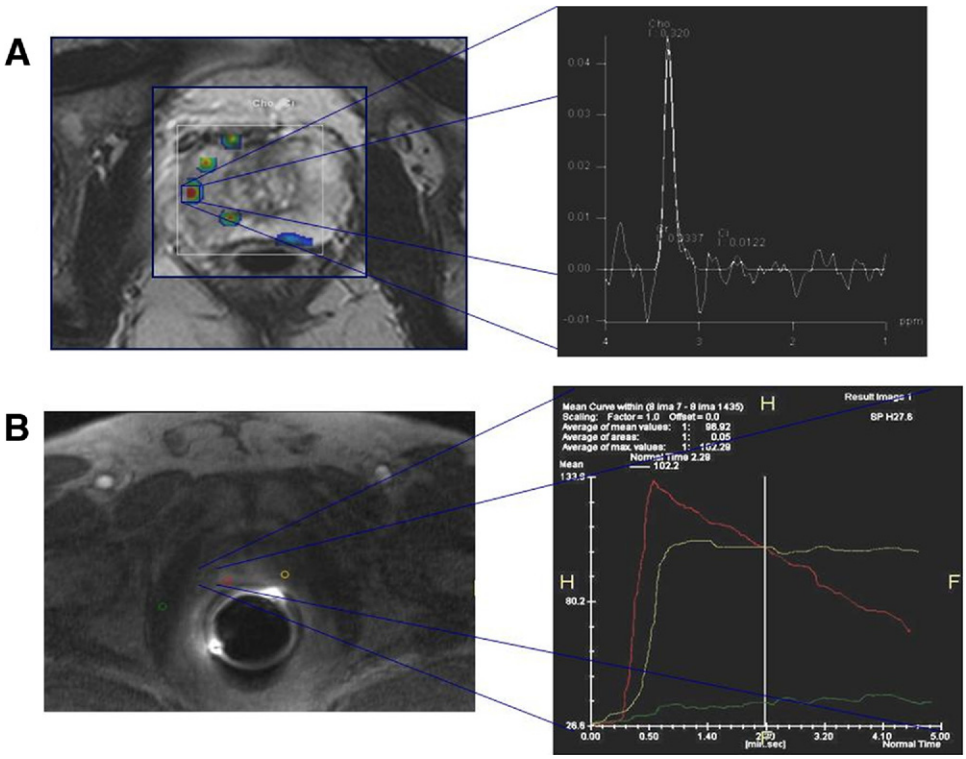

Fig. 1. (A) Spectroscopic analysis at MRI in a case of prostate adenocarcinoma. (B) Dynamic analysis at MRI in a case of prostate adenocarcinoma. (Color version of figure is available online.)

Table 1
Sensitivity, specificity, PPV, NPV, and accuracy of PSA, TRUS, MRSI, and DCEMR in the initial diagnosis of CaP [1,2,20,21,34]

	PSA	TRUS	MRSI	DCEMR
Sensitivity	63%–92%	94%	70%–91%	69%–95%
Specificity	20%–73%	38%	89%–95%	80%–96%
PPV	42%–60%	48%	88%–91%	—
NPV	—	—	74%–95%	—
Accuracy	—	—	79%–96%	77%–92%

ever, biopsy itself has limitations in terms of sensitivity and specificity, and some studies emphasized that sextant biopsies miss out 30% of cancers [11].

Yuen et al. [22,23] referred that combined MRI to MRSI can increase CaP detection in patients at high risk when the cancer is located in the transitional zone or in the anterior peripheral zone, parts of the prostate that are not easily palpable at DRE and not routinely targeted during biopsy.

MRSI could also be useful in the management of patients with a persistently increasing PSA-value and negative prostate biopsies. The probability of positive biopsy in patients with negative DRE and endorectal MRI and PSA values between 5 and 15 ng/ml is 5%–10% at first and second biopsies, and from the second biopsy onwards the risk of positive biopsy decreases (8% at the third biopsy; 5% at the fourth, and 2%–3% at the fifth) [10]. Biopsy strategies with an increased number of random biopsy cores have been proposed to reduce false negative rate. However, saturation biopsy can be associated with increased patient morbidity, and the issue of whether taking more cores results in the detection of more tumors with low-risk characteristics remains controversial. The MRSI should therefore be a useful test when it comes to rule out the presence of tumors, especially in patients with persistent elevation of PSA and previous negative biopsies. It also allows reducing the number of prostate biopsies and, therefore, the distress for patients. Another important advantage of MRSI could be to focus on areas at high risk for CaP before biopsies and to obtain the possibility of targeted biopsies. Yuen et al. [22] performed a study to determine if MRI combined to MRSI can better detect tumor foci in 24 patients with prior negative TRUS biopsy. They concluded that MRSI have the potential to direct biopsy in these patients with a 100% sensitivity, 70.6% specificity, 58.3% PPV, 100% NPV, and 79.2% accuracy for the detection of CaP. We performed (Sciarra et al. under evaluation) the largest randomized prospective study on this topic, showing that in 100 patients with a prior negative prostate biopsy and persistent elevated PSA levels, a combination of a standard 10-core biopsy scheme with an over-sampling strategy in sites targeted to MRSI + DCEMR indications, resulted in significantly higher cancer detection rates (sensitivity 92.6%; specificity 88.8%; PPV 88.7%; NPV 92.7%; accuracy 90%–97%).

In the early diagnosis of CaP and cancer localization, the combined use of MR/MRSI may increase the accuracy of biopsies, reduce false-negative biopsies, and decrease the need for repeated biopsies in the follow-up.

3.2. Possible future recommendation

After a first random biopsy that resulted negative for CaP, in the persistence of clinical suspicious, MRSI detect and localize areas at high risk for CaP (Cho + Cr/Cit ratio) and, therefore, to perform a second targeted biopsy with high PPV and NPV. The term "virtual biopsy" has been coined for the ability of MRSI to provide noninvasive tissue characterization in brain tumors. This optimistic terminology is not yet appropriate for prostatic MRSI. On the contrary, at the present time, MRSI may stratify patients with a high and low probability of a subsequent positive biopsy. Large trials should compare a strategy with MRSI/DCEMR directed biopsies with a saturation biopsy procedure in order to assess their accuracy, and also their morbidity and cost-effectiveness.

3.3. Inflammation and preneoplastic lesions

MRSI and DCEMR may also have a role in the diagnosis of preneoplastic lesions, such as high grade prostatic intraepithelial neoplasia (HGPIN), and also in the definition of the relationship between inflammation, HGPIN, and CaP.

It is too early to define prostate inflammation as a preneoplastic lesion and integrate it in a risk stratification analysis, but recent studies (Sciarra et al. unpublished) compared MRSI and DCEMR features in histologically confirmed prostatic inflammation, HGPIN low grade (LGPC), and high grade (HGPC) CaP. Ninety-six men who underwent combined endorectal MRI + MRSI/DCEMR before TRUS-guided prostate biopsy were divided in 5 groups, depending on histologic response: Group A: control; Group B: inflammation; Group C: HGPIN; Group D: LGPC; Group E: HGPC. At MR imaging, inflammation and HGPIN were not characterized by focal reduction in T2-weighted signal intensity compared with controls. Instead, LGPC and HGPC cases showed focal reduction in T2-weighted signal intensity. At MRSI, there was a significant ($P < 0.05$; F ratio = 3.35) difference in all metabolic assessments between controls (Group A) and the other groups (Groups B, C, D, and E). In particular, all Groups B [choline = 0.3170 ± 0.2580 (95% confidence intervals 0.0459–0.5870); ratio = 1.4570 ± 1.4279 (0.0418–2.9550)], C [choline = 0.3970 ± 0.2988 (0.1680–0.6270); ratio = 1.2140 ± 0.2208 (1.0450–1.3840)], D [choline = 0.2910 ± 0.2506 (0.1080–0.6890); ratio = 2.8130 ± 1.8350 (0.1070–5.7320)], E [choline = 0.7240 ± 0.8549 (0.338–1.786); ratio = 2.4560 ± 1.9751 (0.0035–4.9080)] showed high Cho and ratio values compared with Group A (controls) [choline = 0.0488 ± 0.0494 (0.0074–0.0901); ratio = 0.5520 ± 0.5883 (0.0598–1.0430)]. Group B (inflammation) spectroscopic parameters were very similar to those reported in Group C (HGPIN) and Group D (LGPC). At

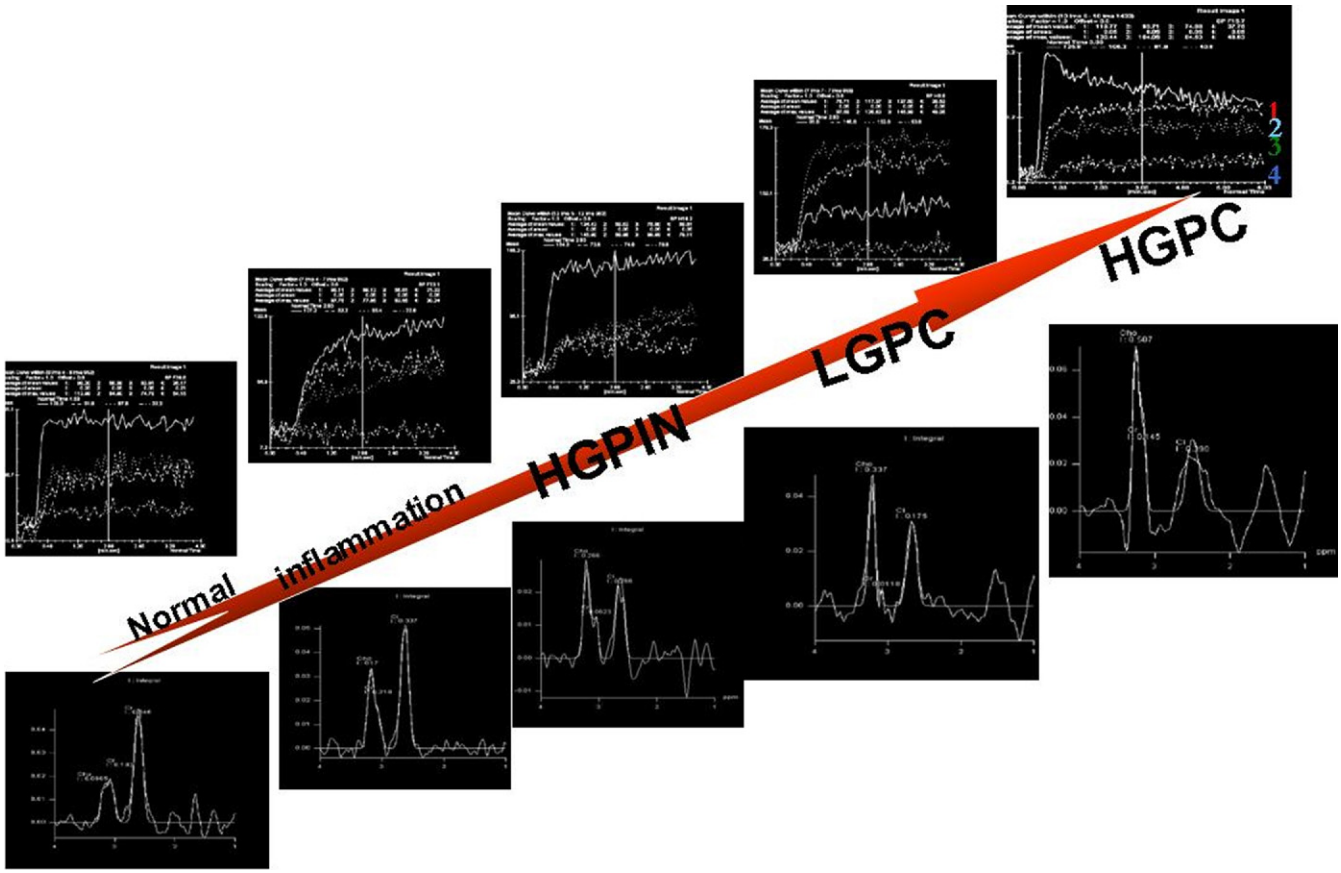

Fig. 2. Spectroscopic MRSI evidence of a link among inflammation, HGPIN, and CaP. (HGPIN = high grade prostatic intraepithelial neoplasia; LGPC = low grade prostate cancer; HGPC = high grade prostate cancer). (Color version of figure is available online.)

DCEMR, there was a significant difference ($P < 0.05$; F ratio = 3.32) in almost all dynamic assessments between controls (Group A) and the other group (Groups B, C, D, and E).

These differences in metabolites concentration at MRSI and DCEMR parameters can be used to support the hypothesis for a link among, inflammation, HGPIN, and CaP (Fig. 2). We must also underline that variability of results were very high, and no conclusive indications can be made.

Also, Horn et al. [24] analyzed HGPIN cases at MRSI, showing choline and ratio levels higher than controls and lower than CaP. These data may be related to an abnormal proliferation, histologically recognized in HGPIN.

3.4. Possible future recommendation

The metabolic assessment obtained at MRSI should be able to characterize preneoplastic lesions at prostate level and the risk for those to progress in CaP. At this time, data in this field are very limited.

3.5. Correlation with Gleason score: Role of MRSI in the determination of tumor aggressiveness

The Gleason score is the most important indicator of CaP aggressiveness. The Gleason score obtained from the biopsy is often different from the Gleason score obtained after radical prostatectomy [25,26]. MRSI can represent a non-invasive significant method for establishing CaP aggressiveness before treatment. Several studies [19,27] indicated that the elevation of choline and the reduction of citrate level are correlated with cancer aggressiveness, and the (Cho + Cr)/Cit ratio is positively correlated with the Gleason score. There is a statistically significant difference in the (Cho + Cr)/Cit ratio when comparing high grade (>7) with low grade (<7) CaP [15]. Moreover, the (Cho + Cr)/Cit index, calculated for the gland, has a positive correlation with the surgical Gleason score [15]. Casciani et al. [15] reported that also tumor volume, measured with MR imaging, has a correlation with increasing Gleason score. There is a limit in the MRSI prediction of CaP aggressiveness: a similar MRSI feature between inflammation and low-grade tumor.

3.6. Possible future recommendation

Considering the significant rate of downgrading for CaP at prostate biopsy, MRSI may help the clinician to correctly evaluate the aggressiveness of CaP in the decision of its

management. At this time, data remain limited and must be supported by larger analysis.

4. CaP management and MRSI/DCEMR

4.1. Informations for surgical management and radiotherapy

An accurate local staging is necessary to make the best treatment decision in patients with localized CaP. The presence of extracapsular extension (ECE) is one of the most important factors influencing the choice of the treatment and the prognosis in patents with CaP.

Using TRUS in local staging for the detection of ECE, accuracy is reported as 58%–86%; sensitivity as 50%–90%; specificity as 46%–91% [28–30]. Jager et al. [31] demonstrated a sensitivity of MRI for a ECE less than 1mm of 15% and a sensitivity for a ECE more than 1mm of 71%, suggesting a possible role of MR imaging in the diagnosis of ECE. Recently, Wang et al. [32] revealed that MRI and MRSI can add more information in the prediction of an organ-confined CaP. Yu et al. [33] indicated that combined MRSI and DCEMR is significantly more reliable than T2-weighted MR imaging for cancer localization and for the determination of the distance between the neurovascular bundle and the prostate capsule. Seitz et al., in their collaborative review article, reported higher sensitivity, specificity, and accuracy values using DCEMR rather than MRSI for tumor staging and localization [34] (Table 2). A higher accuracy of MRSI in tumor mapping has also been shown for planning a radiation therapy. In fact, MRSI can improve DOSE-VOLUME planning in radiotherapy compared with TC or MR, decreasing radiation doses to other sites [19].

4.2. Possible future recommendations

A metabolic mapping of the prostate gland by MRSI may help to obtain a correct tumor localization. The inclusion of MRSI in the actual nomograms may improve prediction of CaP localization and extension, thereby improving patient selection for therapies. The possibility of mapping tumor volume and aggressiveness is a relevant aspect either in a surgical plan (neurovascular bundle preservation; risk of positive surgical margins) or in radiotherapy.

Table 2
Sensitivity, specificity, PPV, NPV, and accuracy of MRSI and DCEMR in the clinical staging and tumor localization [34]

	Tumor localization MRSI	Tumor localization DCEMR	Clinical staging MRSI	Clinical staging DCEMR
Sensitivity	67%–76%	69%–95%	42%–93%	82%–91%
Specificity	57%–69%	80%–96%	81%–89%	90%–95%
PPV	89%–92%	—	81%–93%	87%–91%
NPV	74%–82%	—	50%–86%	91%–95%
Accuracy	74%–79%	81%–93%	74%–85%	90%–96%

4.3. Determination of local recurrence after primary treatment

At present, PSA plays a major role in tumor recurrence or progression diagnosis after radical prostatectomy (RP) [35,36]. A PSA increase within 6–12 months after RP suggests a local recurrence, whereas a PSA increase in a shorter period is usually correlated with the presence of a distant metastasis [37]. All modern imaging modalities (TC, US, RM), which have been employed in the identification of CaP recurrence for a long time, have important limitations. TRUS is considered the most sensitive modality for the identification of local recurrence [38,39]. Some authors reported an overall TRUS-guided biopsy detection rate of 41% with a correct diagnosis of recurrence higher in patients with high PSA levels [40–42]. TC is characterized by a low accuracy in the differentiation of post-RP local recurrence from surgical scar. MR may represent a valid technique for the evaluation of patients with biochemical progression after RP. It is necessary to underline the importance of developing a diagnostic technique to discover an early post-RP local recurrence, considering the efficacy of radiotherapy in the treatment of patients with low-volume recurrence. Some studies have demonstrated that combining MRSI and DCEMR could be a powerful tool for the early diagnosis of post-RP local recurrence [7]. However, only one study revealed the sensitivity and specificity of 1H-MRSI and DCEMR, individually and in combination, for the detection of CaP local recurrence after RP. Sciarra et al. [6] analyzed 70 patients with high risk for local cancer recurrence after RP. Patients were divided in 2 groups: in Group A there were cases subjected to a TRUS-guided biopsy of the post-RP fossa as a validation of MR results; in Group B the PSA level modification after radiation therapy (a reduction >50%) was used as a validation of MR results. In Group B, biopsy was useless because of the size of recurrence. In particular for MRSI, each voxel was categorized as: no solid tissue = Cho + Cr/Ci $<$ 0.2; residual healthy prostatic tissue = Cho + Cr/Ci $>$ 0.2 and $<$ 0.5; probably recurrent CaP = Cho + Cr/Ci $>$ 0.5 and $<$ 1; definitively recurrent CaP = Cho + Cr/Ci $>$ 1.

MR spectroscopy imaging alone and DCE-MRI alone achieved a sensitivity between 71% and 84% (MRSI in Groups A and B), and between 7% and 79% (DCE-MRI in Groups A and B), a specificity between 83% and 88% (MRSI) and between 94% and 100% (DCE-MR). The PPV was 91% to 93% (MRSI) and 96% to 100% (DCE-MR), and the NPV was 56% to 74% (MRSI) and 63% to 67% (DCE-MR). The combined MRSI/DCE-MRI showed a sensitivity of 86% to 87%, a specificity of 94% to 100%, a PPV 96% to 100%, and NPV 75% to 79%. Areas under the curve for MRSI, DC EMR, and combined MRSI + DCEMR were

0.942, 0.931, and 0.964 in Group A and 0.81, 0.923, and 0.94 in Group B.

The lower performance of MRSI in Group B may reflect the problem that the required voxel size for spectroscopic data is larger than that for DCEMR data, and patients in Group B would be predicted to have a smaller volume disease. The result of this study showed that the combined use of MRSI and DCEMR is a valid method for the identification of local CaP recurrence in patients with biochemical progression after RP. In addition, recent studies revealed that MRSI imaging can be useful in the detection of local CaP recurrence after RT. Seitz et al. [34] sustained an association with a sensitivity of 87% and a specificity of 72% between the presence of 3 or more spectroscopic voxels with (Cho + Cr/Cit ratio > 1.5 and local recurrence after RT.

4.4. Possible future recommendation

The determination of a biochemical progression after primary therapy for CaP, as local recurrence or distant progression, is crucial for a correct and early management of patients. MRSI combined with DCEMR may provide a significant and early determination of local recurrence after RRP and RT. The advantage of this new method (also on a histologic determination after biopsy) is its good accuracy for patients with a lower increase of PSA levels and small volume disease.

4.5. Assessment of nerve sparing after RP: Functional aspects of MRI

In recent years, different studies have highlighted the possibility to analyze functional aspects related to the management of CaP at MR. In particular, 3D and 2D MR sequences have been identified among the most useful techniques to define neurovascular bundles (NVB) changes. MR is a powerful tool in the definition of NVB changes after bilateral nerve sparing RP.

Some studies have already analyzed the role of preoperative endorectal MRI when making the decision to preserve or to dissect NVB during RP, or in evaluating the possible erectile dysfunction after bilateral nerve sparing RP [43,44].

In their study, Sciarra et al. [45] attributed to the 3D MRI T2-weighted and 2D MRI T2-weighted images the capacity of defining NVB changes after RRP (Fig. 3). On 53 patients submitted to nerve sparing RRP, they also correlated a MR score based on NVB morphology with the International Index Erectile Functional five-item (IIEF-5) questionnaire.

Erectile dysfunction is one of the most common complications after RP, and to define it, a multidisciplinary approach including the IIEF-5, polysomnography recording nocturnal erections, and color Doppler sonography are employed. In the study from Sciarra et al. [45], a statistically

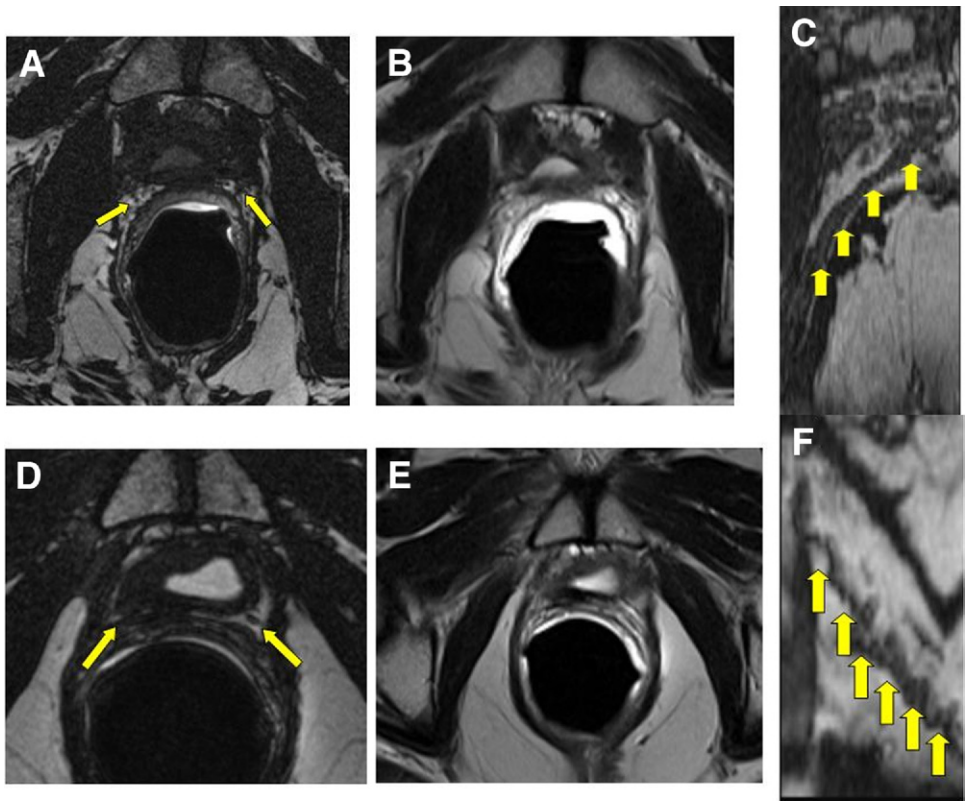

Fig. 3. MRI analysis of NVB after RRP: (A), (B), (C) = regular course (arrows) of neurovascular bundle after RRP; (D), (E), (F) = irregular course (arrows) of neurovascular bundle after RRP. (Color version of figure is available online.)

Table 3
Score to classify NVB changes in signal intensity and anatomical integrity after a bilateral nerve-sparing RRP. In the classification, each category is scored on a point scale where higher values represent a higher grade of NVB alteration on MR images. These points were assigned on the basis of anatomical course delineation for each or both NVBs, adding 0 points for low signal and 1 point when ROI analysis revealed higher NVB signal intensity (when the NVB was identifiable on 3D-T2-ISO images)

0	Normal or quite (nearly) normal (0–2 point range): entire NVB anatomical course bilaterally evaluable (point = 0) ± high signal on T2w (point = 0 or 1 for each NVB)
I	Mild (3–5 point range): NVB anatomical course unilaterally partially evaluable (points = 3) ± high signal on T2w (points = 0 or 1) ± normal or quite normal contralateral NVB (0 or 1 points for high signal intensity)
II	Mild to moderate (6–8 point range): NVB anatomical course bilaterally partially evaluable (points = 6) ± high signal on T2w (points = 0 or 1 for each NVB)
III	Moderate (9–13 point range): NVB anatomical course unilaterally never evaluable, probable resection (points = 9) + 0 points for contralateral NVB entire anatomical course evaluable or 3 points for contralateral NVB anatomical course partially evaluable ± high signal on T2w (points = 0 or 1 for contralateral NVB)
IV	Severe: NVB anatomical course bilaterally never evaluable, probable resection (points = 14)

significant correlation between post-RRP MRI images and IIEF-5 data was obtained ($P = 0.0010$; Spearman's ρ coefficient 0.457; 95% confidential interval: 0.213–0.647). In addition it has been introduced a new MR score that describes the anatomical course integrity using a five-point classification (normal, mild, mild to moderate, moderate, severe) after a nerve sparing RP (Table 3).

4.6. Possible future recommendation

Specific 3D and 2D MRI sequences may help to define the integrity or the damage in NVB after RP. This is an important functional role for MRI, considering the possibility to modulate a sexual rehabilitative program after surgery on the basis of MR results and scores. For this reason, MRI sequences on NVB after RP should be enclosed in the functional postsurgical evaluation of our patients.

4.7. Assessment of response to hormone therapy

Some studies analyzed the detection at MR of tumor volume variation during hormone therapy as prediction of therapeutic response in CaP [46]. Recent studies stressed on the usefulness of combined MR and MRSI imaging in monitoring the response to hormone therapy in patients with CaP. Mueller-Lisse et al. [47] have reported a time-dependent loss of prostatic metabolites during hormone therapy. They obtained a complete loss of (Cho + Cr)/Cit ratio in 25% of patients who had received 4 months of hormone deprivation therapy. Sciarra et al. [48] obtained a normalisation of the ratio (Cho + Cr)/Cit from >1 (pretreatment) to <0.5 (posttreatment), using the 1H-MRSI technique in a patient with an advanced CaP and neuroendocrine differentiation (treated with a combination of complete androgen blockade and somatostatin analogue). MRSI results significantly correlated with PSA and chromogranin A reduction at response to therapy.

4.8. Possible future recommendation

The presence of different targeted medical therapies, which can be proposed at different steps in advanced CaP, sustains the need for an imaging technique able to describe responses in these patients. However, MRSI limits analysis to the prostate gland in a stage where distant metastases are more relevant for the risk of progression and the survival of patients.

5. Conclusions

Several data underline an emerging role of MRI in particular with MRSI but also, in some fields, with DCEMR, as the most sensitive tool for the imaging of CaP. The metabolic evaluation offered by MRSI and the functional dynamic evaluation offered by DCEMR, significantly improve the accuracy of the anatomic imaging of CaP obtained with MR. Future guidelines and recommendations should sustain MRSI and DCEMR in the clinical management of patients with CaP at different levels: in particular, in the initial assessment, reducing the need for more extensive biopsies and directing targeted biopsies; in the definition of a biochemical progression after primary therapy, distinguishing between fibrotic reaction and local recurrence from CaP (Table 4). Large randomized studies demonstrating the usefulness and costs-

Table 4
Possible applications of MRSI in the clinical management of CaP

Phase	Advantages	Competitors
Initial diagnosis	- Identification of areas at elevated risk for CaP so to direct biopsies and re-biopsies	- TRUS - MRI
Planning pre-RRP or RT	- Map of the tumor inside the prostate gland - Map of areas at higher aggressiveness inside the tumor - Reduction of the risk for understaging and undergrading	- Biopsy - TRUS - MRI
Follow-up post-RRP or RT	- Early identification of low volume local recurrences	- Biopsy - TRUS - MRI
Hormonal therapy	- Metabolic evaluation of the local response to hormone therapies - Evaluation of local progression during therapies	- PSA - MRI

RRP = radical prostatectomy; RT = radiotherapy; TRUS = transrectal ultrasonography; PSA = prostate specific antigen; MRI = magnetic resonance imaging.

effectiveness advantage of MRSI/DCEMR in these different setting should be developed.

References

[1] Aus G, Abbou CC, Bolla M, et al. EAU guidelines on prostate cancer. Eur Urol 2005;48:546–51.

[2] Heidenreich A, Aus G, Bolla M, et al. EAU guideline on prostate cancer. European Association of Urology. Eur Urol 2008;53:68–80.

[3] Choyke PL. Imaging of prostate cancer. Abdm Imaging 1995;20: 505–15.

[4] Stamey T. Making the most out of six systematic sextant biopsies. Urology 1995;45:2–12.

[5] Hernandez J, Thompson IM. Prostate-specific antigen: A review of the validation of the most commonly used cancer biomarker. Cancer 2004;101:894–904.

[6] Sciarra A, Panebinanco V, Salciccia S, et al. Role of dynamic contrast-enhanced magnetic resonance imaging and proton MR spectroscopic imaging in the detection of local recurrence after radical prostatectomy for prostate cancer. Eur Urol 2008;54:589–600.

[7] Kirkham AP, Emberton M, Allen C. How good is MRI at detecting and characterizing cancer within the prostate? Eur Urol 2006;50: 1163–75.

[8] Anastasiadis AG, Lichy MP, Nagele U, et al. MRI-guided biopsy of the prostate increases diagnostic performance in men with elevated or increasing PSA levels after previous negative TRUS biopsies. Eur Urol 2006;50:738–49.

[9] Rajesh A, Coakley FV, Khrhanewicz J. 3D spectroscopic imaging in the evaluation of prostate cancer. Clin Radiol 2007;62:921–9.

[10] Comet-Batle J, Vilanova-Busquests JC, Saladiè-Roig JM, et al. The Value of endorectal MRI in the early Diagnosis of prostate cancer. Eur Urol 2003;44:201–8.

[11] Hricak H. MR imaging and MR spectroscopic imaging in the pretreatment evaluation of prostate cancer. Br J Radiol 2005;78:103–11.

[12] Heuck A, Scheidler J, Sommer B, et al. MR imaging of prostate cancer. Radiologe 2003;43:464–73.

[13] Hersh MR, Knapp EL, Choi J. Newer imaging modalities to assess tumor in the prostate. Cancer Control 2004;11:353–7.

[14] Rajesh A, Coakley FV. MR imaging and MR spectroscopic imaging of prostate cancer. Magn Reson Imaging Clin N Am 2004;12:557–79.

[15] Casciani E, Gualdi G. Prostate cancer: Value of magnetic resonance spectroscopy 3D chemical shift imaging. Abdom Imaging 2006;31: 490–9.

[16] Shukla-Dave A, Hricak H, Eberhardt SC, et al. Chronic prostatitis: MR imaging and 1H MR spectroscopic imaging findings-initial observations. Radiology 2004;231:717–24.

[17] Casciani E, Polettini E, Bertini L, et al. Granulomatous prostatitis: A pitfall in endorectal MR imaging and 3D MR spectroscopic imaging. Eur J Radiol 2005;54:111–4.

[18] Kaji Y, Kurhanewicz J, Hricak H, et al. Localizing prostate cancer in the presence of post-biopsy changes on MR images: Role of proton MR spectroscopic imaging. Radiology 1998;206:785–90.

[19] Sciarra A, Salciccia S, Panebianco V. Proton spectroscopic and dynamic contrast-enhanced magnetic resonance: A modern approach in prostate cancer imaging. Eur Urol 2008;54:485–8.

[20] Manenti G, Squillaci E, Carlani M, et al. Magnetic resonance imaging of the prostate with spectroscopic imaging using a surface coil. Initial clinical experience. Radiol Med (Torino) 2006;111:22–32.

[21] Bloch BN, Furman-Haran E, Helbich TH, et al. Prostate cancer: Accurate determination of extracapsular extension with high-spatial-resolution dynamic contrast-enhanced and T2-weighted MR imaging initial results. Radiology 2007;245:176–85.

[22] Yuen JS, Thng CH, Tan PH, et al. Endorectal magnetic resonance imaging and spectroscopic for the detection of tumor foci in men with prior negative transrectal ultrasound prostate biopsy. J Urol 2004; 171:1482–6.

[23] Amsellem-Ouazana D, Younse P, Conquy S, et al. Negative prostatic biopsies in patients with High risk of prostate cancer. Eur Urol 2005;47:582–6.

[24] Horn JJ, Coakley FV, Simko JP, et al. HGPIN in patients with prostate cancer; MR and MR spectroscopic imaging features: Initial experience. Radiology 2007;242:483–9.

[25] Cookson MS, Fleshner NE, Soloway SM, et al. Correlation between Gleason score of needle biopsy and radical prostatectomy specimens: Accuracy and clinical implications. J Urology 1997;157:559–62.

[26] Steinberg MD, Sauvageot J, Piantadosi S, et al. Correlation of prostate needle biopsy and radical prostatectomy Gleason grade in academic and community settings. Am J Surg Pathol 1997;21:566–76.

[27] Zakian KL, Sircar K, Hricak H, et al. Correlation of proton MR spectroscopic imaging with Gleason score based on step-section pathologic analysis after radical prostatectomy. Radiology 2005;234: 804–14.

[28] Smith JA Jr, Scardino PT, Resnick MI, et al. Transrectal ultrasound versus digital rectal examination for the staging of carcinoma of the prostate: Results of a prospective, multi-institutional trial. J Urol 1997;157:902–6.

[29] Cornud F, Belin X, Piron D, et al. Color Doppler-guided prostate biopsies in 591 patients with an elevated serum PSA level: Impact on Gleason score for nonpalpable lesions. Urology 1997;49:709–15.

[30] Wilkinson BA, Hamdy FC. State-of-the-art staging in prostate cancer. BJU Int 2001;87:423–30.

[31] Jager JG, Ruijter ET, van de Kaa CA, et al. Local staging of prostate cancer with endorectal MR imaging: Correlation with histopathology. AJR 1996;166:845–50.

[32] Wang L, Hricak H, Kattan KW, et al. Prediction of organ confined prostate cancer. Incremental value of MR imaging and MR spectroscopic imaging to staging nomograms. Radiology 2006;238:597–603.

[33] Yu KK, Scheidler J, Hricak H, et al. Prostate cancer: Prediction of extracapsular extension with endorectal MR imaging and three-dimensional proton MR spectroscopic imaging. Radiology 1999;213:481–8.

[34] Seitz M, Shukla-Dave A, Bjartell A, et al. Functional magnetic resonance imaging in prostate cancer. Eur Urol 2009 [Epub ahead of print].

[35] Yan Y, Carvalhal GF, Catalona WJ, et al. Primary treatment choices for men with clinically localized prostate carcinoma detected by screening. Cancer 2000;88:1122–30.

[36] Sakai I, Harada K, Kurahashi T, et al. Usefulness of the nadir value of serum prostate-specific antigen measured by an ultrasensitive assay as a predictor of biochemical recurrence after radical prostatectomy for clinically localized prostate cancer. Urol Int 2006;76:227–31.

[37] Neulander EZ, Soloway MS. Failure after radical prostatectomy. Urology 2003;61:30–6.

[38] Prando A, Kurhanewicz J, Borges AP, et al. Prostatic biopsy directed with endorectal MR spectroscopic imaging findings in patients with elevated prostate specific antigen levels and prior negative biopsy findings: Early experience. Radiology 2005;236:903–10.

[39] Futterer JJ, Heijmink SW, Scheenen TW, et al. Prostate cancer localization with dynamic contrast-enhanced MR imaging and proton MR spectroscopic imaging. Radiology 2006;241:449–58.

[40] Shekarriz B, Upadhyay J, Wood DP Jr. Vesicourethral anastomosis biopsy after radical prostatectomy: Predictive value of prostate-specific antigen and pathologic stage. Urology 1999;54:1044–8.

[41] Silverman JM, Krebs TL. MR imaging evaluation with a transrectal surface coil of local recurrence of prostatic cancer in men who have undergone radical prostatectomy. AJR Am J Roentgenol 1997;168: 379–85.

[42] Raj GV, Partin AW, Polascik TJ. Clinical utility of indium 111-capromab pendetide Immunoscintigraphy in the detection of early, recurrent prostate carcinoma after radical prostatectomy. Cancer 2002;94:987–96.

[43] Hricak H, Wang L, Wei DC, et al. The role of preoperative endorectal magnetic resonance imaging in the decision regarding whether to preserve or resect neurovascular bundles during radical retropubic prostatectomy. J Urol 2005;173:416.

[44] Lee SE, Hong SK, Han JH, et al. Significance of neurovascular bundle formation observed on preoperative magnetic resonance imaging regarding postoperative erectile function after nerve-sparing radical retropubic prostatectomy. Urology 2007;69: 510–4.

[45] Panebianco V, Sciarra A, Salciccia S, et al. 2D and 3D T2-weighted MR sequences for the assessment of neurovascular bundle changes after nerve-sparing radical retropubic prostatectomy with erectile function correlation. Eur Radiol 2009;19:220–9.

[46] D'Amico AV, Halabi S, Tempany C, et al. Tumor volume changes on 1.5 Tesla endorectal MRI during neoadjuvant androgen suppression therapy for higher risk prostate cancer and recurrence in men treated using radiation therapy results of the phase II CALGB 9682 study. Int J Radiat Oncol Biol Phys 2008;71:9–15.

[47] Mueller-Lisse UG, Swanson MG, Vigneron DB, et al. Hormone ablation of localized prostate cancer: Time dependent therapy effects on prostate metabolism detected by 3D 1H MR spectroscopy. Magn Reson Med 2001;46:49–57.

[48] Sciarra A, Panebianco V, Ciccariello M, et al. Complete response to the combination therapy with androgen blockade and somatostatin analogue in a patient with advanced prostate cancer. Eur Urol 2008; 53:652–5.